

1 Article

2 Radar Detection of Fluctuating Target in Heavy- 3 tailed Clutter Using TBD

4 Jie Gao ^{1,2,*}, Jinsong Du ¹ and Wei Wang ^{1,2}

5 ¹ Shenyang Institute of Automation, Chinese Academy of Sciences, Shenyang 110016, China; jsdu@sia.cn

6 ² University of Chinese Academy of Sciences, Beijing 100049, China; wangwei2@sia.cn

7 * Correspondence: gaojie@sia.cn; Tel.: +86-24-8360-1084

8

9 **Abstract:** This paper considers the detection of fluctuating target in heavy-tailed clutter through the
10 use of dynamic programming based on track-before-detect (DP-TBD) in radar systems. The clutter
11 is modeled in terms of K-distribution, which can be widely used to describe non-Gaussian clutter
12 received from high-resolution radars and radars working at small grazing angle. Swerling type 1 is
13 considered to describe the target fluctuation between scans. Conventional TBD techniques suffer
14 from significant performance loss in heavy-tailed environments due to the more frequent
15 occurrences of target-like outliers. In this paper, we resort to DP-TBD algorithm based on prior
16 information, which can enhance the detection performance by using the environment and target
17 fluctuating information during the integration process of TBD. Under non-Gaussian background,
18 the expressions of the likelihood ratio merit function for Swerling type 1 target are derived first.
19 However, the closed analytical form of the merit function is difficult to be obtained. In order to
20 reduce the complexity of evaluating the merit function and the computational load, an efficient
21 approximation method as well as a two-stage detection approach is proposed and used in the
22 integration process. Finally, several numerical simulations of the new strategy and the comparisons
23 are presented to verify that the proposed algorithm can improve the detection performance,
24 especially for fluctuating target in heavy-tailed clutter.

25 **Keywords:** target detection; radar systems; K-distributed clutter; heavy-tailed; Swerling target;
26 track-before-detect (TBD)

27

28 1. Introduction

29 The detection of fluctuating target with low signal-to-clutter ratio (SCR) is of significant
30 importance in radar systems. Conventional detecting and tracking algorithms use thresholded
31 detection as input. Target with low signal-to-clutter ratio is often lost due to the information is
32 irreversibly discarded after thresholding. Multi-frame integration is an effective strategy used in
33 radar applications to detect dim target by integrating signal returns over multiple consecutive scans.
34 In the presence of moving target, multi-frame integration requires track-before-detect (TBD)
35 techniques to correctly correlate data over time.

36 Dynamic programming based on TBD (DP-TBD) is one of the TBD techniques [1,2], which has
37 attracted extensive attention for the advantages of simplicity and needing less information. It
38 transforms the integration into an optimal estimation of the physically admissible trajectory by
39 maximal integration value of the merit function, which is a kind of multi-frame test statistic. DP-TBD
40 can detect target of arbitrary motion form and has been widely applied to several kinds of sensors
41 [3,4]. In order to solve the problem of high-dimensional maximization under multi-target
42 environment, a novel partition method to cluster targets into well separate groups was proposed
43 in[5]. In [6,7], the track formation procedure with successive track cancellation (STC) was described
44 to overcome the performance loss when targets are closely-spaced. Meanwhile, research on the merit
45 function of DP-TBD has also been widely carried out in recent years. In [8-10], the expressions for the
46 log-likelihood ratio (LLR), which can better discriminate clutter-plus-target measurements from

47 clutter only measurements, were derived and used. In addition, a low-complexity power-efficient
48 TBD procedure, where the generalized likelihood ratio test (GLRT) was solved using a Viterbi-like
49 tracking algorithm, was proposed in [11]. To reduce the big computational burden of DP-TBD,
50 computationally efficient DP-TBD algorithms were derived in [12] and [13] respectively.

51 The above quoted papers on DP-TBD techniques always assumed that the background is
52 Gaussian distributed with known power. However, for high resolution radars and radars at small
53 grazing angle, the Gaussian assumption may or may not be adequate. In this case, more heavy-tailed
54 background models should be considered in the real world. Weibull distribution, log-normal
55 distribution and K-distribution are the commonly Compound-Gaussian background models used in
56 radar communities. This paper is mainly concerned with K-distribution, which is widely used in high
57 resolution radar detection systems. K-distribution [14,15] was derived from a paper by Eric Jakeman
58 and Peter Pusey (1978) who used it to model microwave sea echo. It has been found to be a suitable
59 model for heavy-tailed background in radar systems [16], since it provides an excellent agreement
60 between theoretical and experimental data. K-distribution also arises as the consequence of a
61 statistical or probabilistic model used in Synthetic Aperture Radar (SAR) imagery.

62 As the signal strength may change from scan to scan, these fluctuations should be taken into
63 account when building the measurement models. Swerling family of target amplitude fluctuation
64 models are commonly used to capture the RCS changes over time [17]. Swerling target of types 0 can
65 be used to model a target with constant RCS, while Swerling target of types 1 is used to model a
66 target whose RCS fluctuates according to the exponential density in radar systems.

67 Target detection in K-distributed background is more challenging than in Gaussian or Rayleigh
68 distributed background due to the higher likelihood of target-like outliers, especially for fluctuating
69 target. Besides, it is inefficient and computationally costly to carry out accurate search for all the
70 discrete states, as the surveillance region is much larger than the size of a target, such as radar target
71 detection. In this paper, attention is devoted to the detection of Swerling target of type 1 in a
72 surveillance region characterized by K-distributed background through the use of DP-TBD.
73 Moreover, by employing two-stage detection approach, the proposed algorithm is able to achieve
74 further computational reduction. The main contributions of this paper are given as below:

75

- 76 1. In order to limit complexity while still retain the benefits of DP-TBD, we resort to two-stage
77 detection process with different resolution cells.
- 78 2. For typical non-Gaussian distributed clutter (K-distribution) and typical target amplitude
79 fluctuation model (Swerling 1), the DP-TBD algorithm based on prior information is proposed.
80 By using the likelihood ratio merit function in DP integration, the performance loss produced
81 by the "heavy-tailed" clutter measurements can be reduced.
- 82 3. An efficient but accurate approximation method is proposed to reduce the complexity of
83 evaluating the merit function.

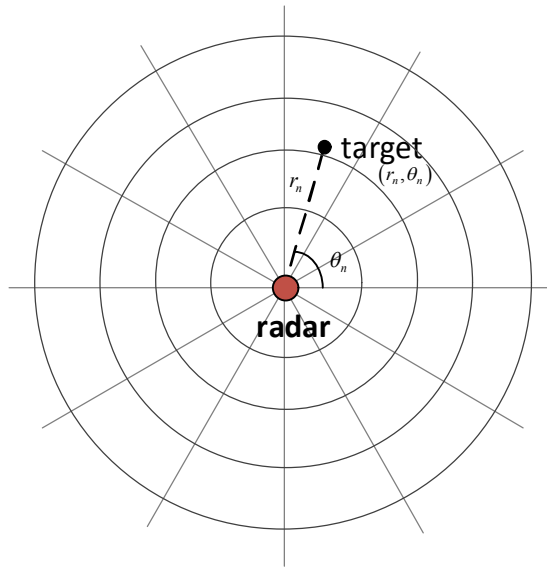
84

85 The remainder of this paper is organized as follows: Section 2 presents the notations and system
86 models. In Section 3, two-stage detection approach is proposed at first, the expressions of the
87 likelihood ratio merit function are derived in K-distributed clutter background for Swerling target of
88 types 1, the implementation issues of the merit function are also discussed. Simulation results are
89 showed by comparing different DP-TBD strategies in Section 4 and Section 5 provides some
90 conclusions.

91

92 2. Models and Notations

93 2.1. Kinematic Model



94 **Figure 1.** Radar surveillance region illustration.

95 As shown in Figure 1, we assume that there is only one target in the surveillance region, whose
96 kinematic state at scan n is denoted by the vector s_n . The kinematic vector s_n is specified by

$$s_n = [r_n, \theta_n]^T \in \mathcal{R}^2, \quad 1 \leq n \leq N \quad (1)$$

97 where T denotes matrix transpose, r_n and θ_n denote the range and azimuth measurement
98 respectively, \mathcal{R}^2 denotes the two-dimensional state space and N denotes the number of
99 consecutive frames processed in a DP-TBD integration batch. The evolution of the target state is
100 modeled by the linear process as

$$s_n = F s_{n-1} + w_n \quad (2)$$

101 The term w_n is the process noise, F is the transition matrix.

102 Every real target must comply with some physical constrains on its kinematics, such as the
103 maximum target velocity considered in this paper. The radial and tangential velocity can be
104 calculated by two successive scans, which are given by

$$\begin{aligned} v_{n-radial} &= \frac{r_n - [r_{n-1} \times \cos(\theta_n - \theta_{n-1})]}{T} \\ v_{n-tangential} &= \frac{r_{n-1} \times \sin(\theta_n - \theta_{n-1})}{T} \end{aligned} \quad (3)$$

105 where T denotes the time interval between successive scans.

106 2.2. Measurement Model

107 The measurement data consists of M_r cells in the range-dimension and M_θ cells in the
108 azimuth-dimension. If no target exists (hypothesis H_0), the (i, j) th recorded resolution cell, $z_n(i, j)$
109 $1 \leq i \leq M_r, 1 \leq j \leq M_\theta$, at scan n can be expressed as

$$z_n(i, j) = c_n(i, j) \quad (4)$$

110 while in the presence of a target (hypothesis H_1), the recorded resolution cell $z_n(i, j)$ can be
111 expressed as

$$z_n(i, j) = A_n + c_n(i, j) \quad (5)$$

112 where A_n denotes a complex fluctuated amplitude measurement from the target, and $c_n(i, j)$
 113 denotes the K-distributed clutter, which is assumed in this paper.

114 Swerling 1 fluctuation model supposes that returned signal power per pulse is to be constant
 115 during a single scan, but to fluctuate independently from scan to scan. The probability density
 116 function (PDF) of the Swerling 1 target amplitude A_n is given by

$$p(A_n) = \frac{2A_n}{\bar{\sigma}} \exp\left(-\frac{A_n^2}{\bar{\sigma}}\right) \quad (6)$$

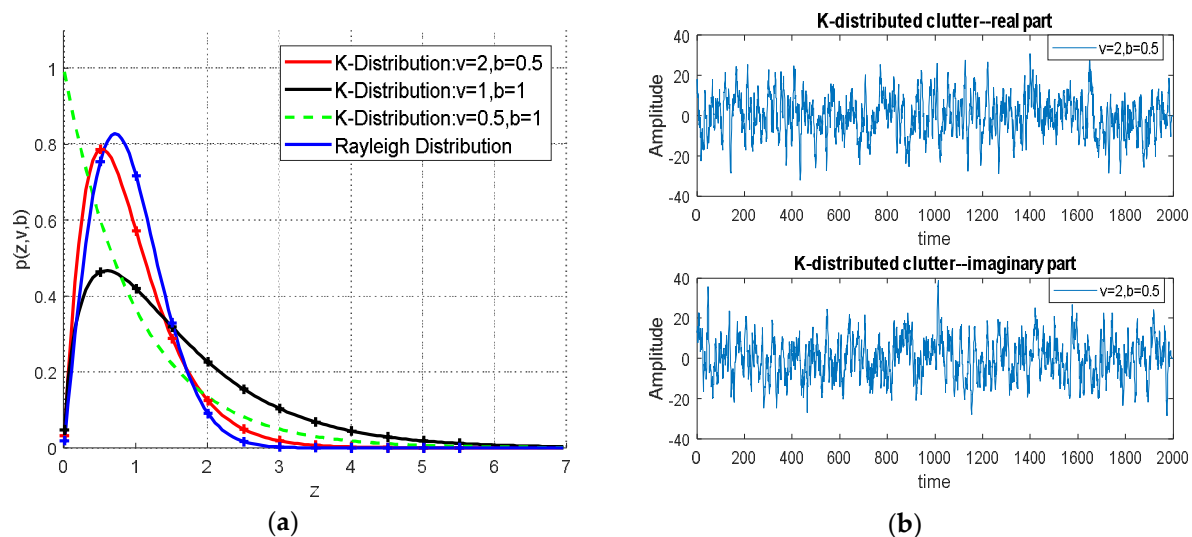
117 with $\bar{\sigma}$ being the mean squared target amplitude.

118 2.3. K-distributed Clutter Model

119 The K-distributed model is proposed as a model for radar clutter in this paper, which has the
 120 probability density function as

$$p(z, v, b) = \frac{2}{b \Gamma(v)} \left(\frac{z}{2b}\right)^v K_{v-1}\left(\frac{z}{b}\right) \quad (7)$$

121 In formula, $\Gamma(\cdot)$ denotes the Gamma function and $K_{v-1}(\cdot)$ denotes the modified Bessel function
 122 of the second kind, z is the clutter amplitude, b is scale parameter which describes the intensity of
 123 the clutter, v is the shape parameter which determines the shape of the distribution function. For
 124 $v \rightarrow \infty$, the K-distribution turns into the Rayleigh distribution. PDFs of K- and Rayleigh-
 125 distributions are shown in Figure2 (a) while the K-distributed clutter ($v=2, b=0.5$) is shown in
 126 Figure2 (b).



127 **Figure 2.** K-distribution (a).PDFs of K- and Rayleigh- distribution for various shape and
 128 scale parameters; (b).K-distributed clutter including real part and imaginary part.

129 The substitution is used as $a_n = |z_n|$, which denotes the amplitude measurement, so that (7) can
 130 be rewritten as

$$p(a_n) = \frac{4a_n^\alpha}{\beta^{(\alpha+1)/2} \Gamma(\alpha)} K_{\alpha-1}\left(\frac{2a_n}{\beta^{1/2}}\right) \quad (8)$$

131 where $\alpha=v$ denotes the shape parameter, $\beta = 4b^2$ denotes the scale parameter.

132 Meanwhile, K-distribution can also be viewed as a Rayleigh distribution modulated by a
133 Gamma distribution for convenience

$$p(a_n) = \int_0^{+\infty} p(a_n|\eta)p(\eta)d\eta \quad (9)$$

134 where

$$p(a_n|\eta) = \frac{2a_n}{\eta} \exp\left(-\frac{a_n^2}{\eta}\right) \quad (10)$$

$$p(\eta) = \frac{\eta^{\alpha-1}}{\beta^\alpha \Gamma(\alpha)} \exp\left(-\frac{\eta}{\beta}\right) \quad (11)$$

135 3. Development of the Proposed Strategies

136 DP-TBD algorithm decomposes the integration among N successive scans into N sub-processes.
137 The n th sub-process contains all the measurements up to scan n . Target can be detected and tracked
138 by calculating the maximum of the energy integration value through a recursive model, which could
139 be expressed as:

$$V(s_n) = I(s_n) \nabla \max_{s_{n-1} \in \tau(s_n)} [V(s_{n-1})] \quad (12)$$

$$\Psi(s_n) = \arg \max_{s_{n-1} \in \tau(s_n)} [V(s_{n-1})] \quad (13)$$

140 where $I(s_n)$ is defined as the merit function at scan n ; $V(s_{n-1})$ is defined as the maximal
141 integration value of all the admissible trajectories; $\tau(s_n)$ is a collection of states at scan n for which
142 a transition to s_n is possible, and it can be obtained by the location and maximum velocity of the
143 target; ∇ is the operator of integration; $\Psi(s_n)$ is the retracing function, indicating the best state of
144 the previous scan, which makes the integration value reach its maximum.

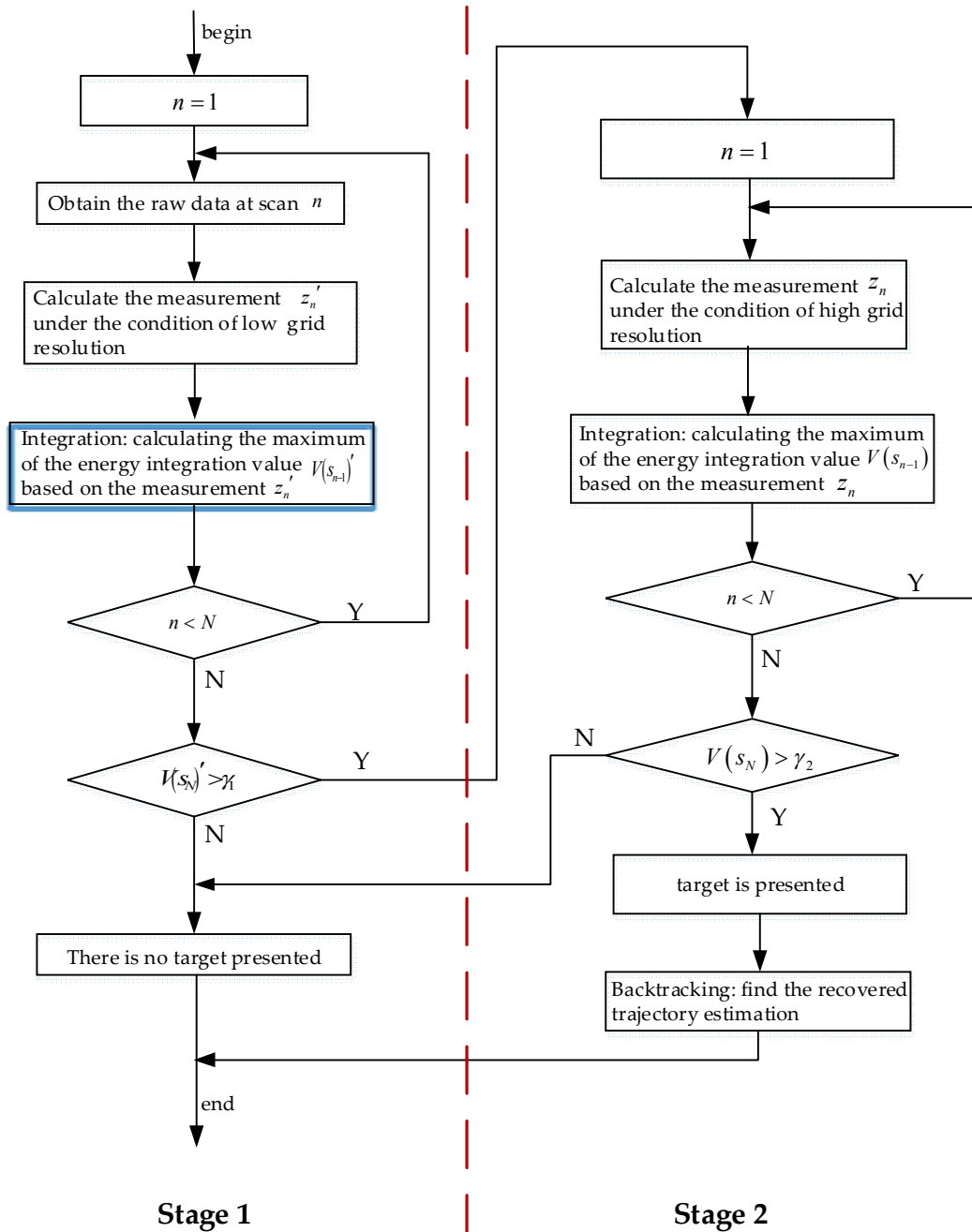
145 In summary, DP-TBD implements the equivalent of an exhaustive search in an efficient manner
146 by enumerating and valuing all physical admissible state sequences, finally returning the state
147 sequences whose final maximal integration value $V(s_N)$ exceeds a given detection threshold γ , i.e.

$$V(s_N) > \gamma \quad (14)$$

148 There are mainly two problems throughout the process. Firstly, the computational complexity
149 of DP-TBD is unaffordable in the presence of high-mobility target when the number of resolution
150 elements is large. The discretization of state space is always based on the sensor's resolution so as to
151 make full use of the measurements and achieve possibly accurate estimates. In this situation,
152 strategies hardly lead to real-time implementable schemes, even resorting to dynamic programming
153 algorithm. In order to reduce the burden of computation, a two-stage detection approach is proposed
154 in this work. Secondly, most of the previous work on DP-TBD assumed that the background model
155 would be Rayleigh or Gaussian distribution with a known power. Such assumptions may or may not
156 be adequate, as in real world, more heavy-tailed background model is often encountered than
157 expected. To improve the detection performance, we propose a novel DP-TBD algorithm based on
158 the prior information to solve the aforementioned problem. In this paper, the merit function is set to
159 be likelihood ratio under both target-present hypothesis and null-target hypothesis in a surveillance
160 region which characterized by K-distributed background, and the simulated data would be tested for
161 presenting the performance.
162

163 3.1. Two-stage Detection Approach

164 Since the surveillance region is much larger than the part of the measurements which are related
 165 to the target, it is inefficient and computational costly to carry out accurate search based on all the
 166 sensor's resolution for the discrete states. In order to reduce the computational load, while still retain
 167 the benefits of TBD, here we resort to a two-stage detection approach which is illustrated in Figure 3.



168 **Figure 3.** The flowchart of the two-stage detection approach.

169 At stage 1, we first obtain the raw data at scan n , and roughly calculate the measurement z'_n
 170 under the condition of low grid resolution. The target states are estimated by searching discrete
 171 grids with larger cell size based on the DP integration. After N times loop, the maximum of the
 172 energy integration value $V'(s_N)$ at scan N could be got by the process. For single target model, the
 173 maximum integration value $V'(s_N)$ which exceeds detection threshold γ_1 is used to determine the

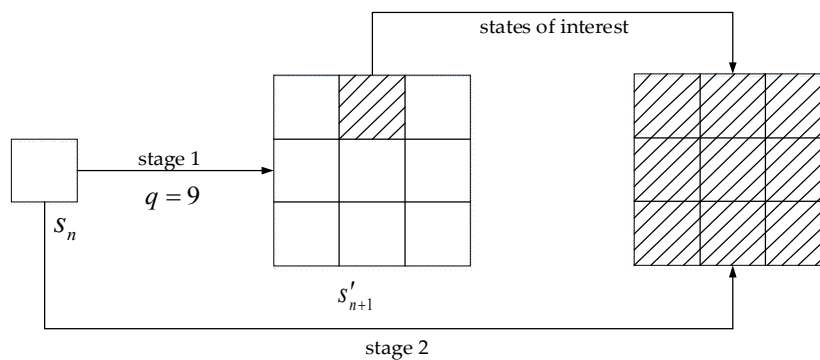
174 existence of target. If there is a target presented in the surveillance region, we could refine the target
175 trajectory in stage 2.

176 In order to obtain a more accurate estimate, stage 2 is employed to recalculate the
177 measurements under the high grid resolution condition. Once the maximum integration value
178 $V(s_N)$ exceeds the detection threshold γ_2 , the estimation of final target trajectory can be obtained
179 by backtracking. For each estimated the state \hat{s}_n , we have :

$$\hat{s}_{n-1} = \psi(\hat{s}_n), \text{ for } n = N, \dots, 1 \quad (15)$$

180 So the recovered trajectory estimate is $\hat{S}_N = \{\hat{s}_1, \dots, \hat{s}_N\}$.

181 The surveillance region is divided into $M_r \times M_\theta$ grid cells based on the resolution of the radar
182 system, i.e., Δr and $\Delta \theta$, where M_r and M_θ denote the number of cells in range and azimuth,
183 respectively. To realize the target search with larger cell size, the state space is re-discretized by
184 $\Delta r'$ and $\Delta \theta'$ to obtain $M'_r \times M'_\theta$ grid cells at first. As shown in figure 4, all the measurements and
185 DP integrations are processed in stage 1 based on the new state space, which may get a roughly
186 target trajectory by less computation. Then in stage 2, DP integration concentrates on the part of
187 states which are indicated by stage 1. As calculations of less meaningful states could be avoided, the
188 computational costs will become more reasonable.



189 **Figure 4.** Illustration of possible transition state collection during the two-stage DP integration.

190 3.2. Derivation and Implementation of the Merit Function

191 Combined (6), PDF for the Swerling 1 target in K-distributed clutter is given by

$$p(a_n | \eta, s_n) = \frac{2a_n}{\eta + \bar{\sigma}} \exp\left(-\frac{a_n^2}{\eta + \bar{\sigma}}\right) \quad (16)$$

192 and $p(a_n | s_n)$ can be derived by marginalizing over η since η is random, i.e.

$$\begin{aligned} p(a_n | s_n) &= \int_0^\infty p(a_n | \eta, s_n) p(\eta) d\eta \\ &= \int_0^\infty \frac{2a_n}{\eta + \bar{\sigma}} \exp\left(-\frac{a_n^2}{\eta + \bar{\sigma}}\right) \frac{\eta^{\alpha-1}}{\beta^\alpha \Gamma(\alpha)} \exp\left(-\frac{\eta}{\beta}\right) d\eta \\ &= \frac{2a_n}{\beta^\alpha \Gamma(\alpha)} \int_0^\infty \frac{\eta^{\alpha-1}}{\eta + \bar{\sigma}} \exp\left(-\frac{a_n^2}{\eta + \bar{\sigma}}\right) \exp\left(-\frac{\eta}{\beta}\right) d\eta \\ &= \frac{2a_n}{\beta^\alpha \Gamma(\alpha)} \int_0^\infty f(\eta) d\eta \end{aligned} \quad (17)$$

193 where the integrand $f(\eta)$ is given by

$$f(\eta) = \frac{\eta^{\alpha-1}}{\eta + \bar{\sigma}} \exp\left(-\frac{a_n^2}{\eta + \bar{\sigma}} - \frac{\eta}{\beta}\right) \quad (18)$$

194 Substituting (8) and (17) into the expression of merit function $I(s_n)$ at scan n , $I(s_n)$ can be
195 written as

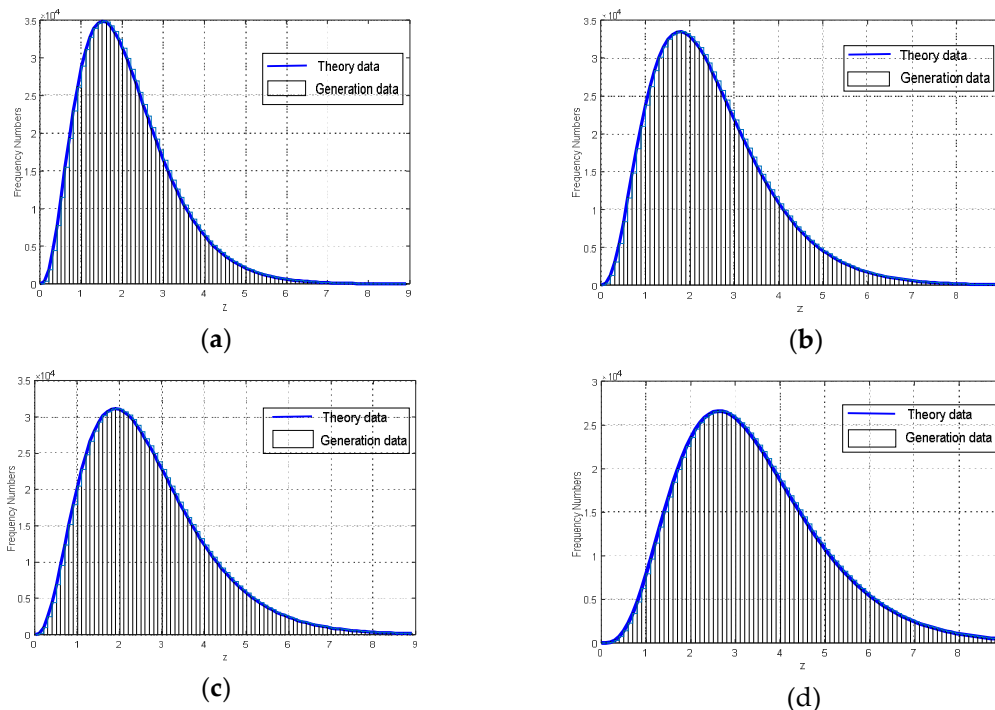
$$\begin{aligned} I(s_n) &= \ln\left(\frac{p(a_n|s_n)}{p(a_n)}\right) \\ &= \ln\left(\frac{a_n^{-\alpha+1} \beta^{(-\alpha+1)/2} \int_0^\infty f(\eta) d\eta}{K_{\alpha-1}(2a_n/\beta^{1/2})}\right) \end{aligned} \quad (19)$$

196 Although the integrand $f(\eta)$ in (18) has no closed-form solution, it can be evaluated with
197 reasonable accuracy by using the trapezoidal rule, i.e.

$$\int_0^\infty f(\eta) d\eta = \sum_{i=1}^{N_{sa}} \frac{f(\eta_i) + f(\eta_{i+1})}{2} \delta_i \quad (20)$$

198 where $f(\eta_i)$ is sample point drawn from the time interval δ_i , δ_i is a sampling interval which is
199 short enough to cover the effective support of $f(\eta)$, N_{sa} denotes the number of sample points.

200 The sample points can be obtained by either deterministic sampling with a uniform grid or
201 stochastic importance sampling. Since the integrand $f(\eta)$ may tend quickly towards ∞ when
202 $\eta \rightarrow 0$, while tend slowly towards 0 when $\eta \rightarrow \infty$. A reasonable approximation obtained by
203 deterministic uniform grid sampling or stochastic importance sampling is difficult to carry out. A
204 grid with variable resolution method was proposed in[18] to approximate merit function which also
205 leads to high computational complexity.



206 **Figure 5.** Histogram of generation data and theory PDF data with SCR=15dB (a). $\alpha=2$ and $\beta=1$; (b).
207 $\alpha=3$ and $\beta=2$; (c). $\alpha=5$ and $\beta=2$; (d). $\alpha=10$ and $\beta=5$;

208 In order to reduce the complexity of approximation, we could possibly circumvent these
 209 problems by generating a lookup table offline with sample points using a uniform grid. The number
 210 of sample points with uniform grid is large enough to approximate the integrand $f(\eta)$ accurately.
 211 Based on the lookup table, this calculating method trades little cost of precision and memory space
 212 to a great improve on running speed in calculation. Histogram of generation data and theory PDF
 213 are shown in Figure 5 for Swerling targets types 1 with different parameters. According to Figure 5,
 214 we conclude that the approximation error is negligible.

215 Note that the K-distribution shape parameter α , the scale parameter β are supposed to be
 216 known in the derivation of merit function. In the case where the background is significantly heavy-
 217 tailed and the parameters are unknown, we should estimate the parameters first, which can be
 218 obtained through a numerical maximization of the likelihood function. Since the maximum
 219 likelihood techniques require numerical optimization routines and evaluation of Bessel functions,
 220 they are computationally intensive and therefore inappropriate for evaluation of large data sets.
 221 Abraham [19] recommended a moment estimators based on the first and second moments, which can
 222 be used as our estimator in this work.

223 4. Simulation

224 In this paper, the detection performances of conventional DP-TBD and proposed strategy for
 225 Swerling type 1 target are assessed. We assume that the measurement noise satisfies K-distribution,
 226 each measurement frame consists of $M_r \times M_\theta = 180 \times 90$ resolution cells. The number of frames
 227 processed in a DP batch is $N = 6$, while the number of possible state transition in a scan is $q=9$. This
 228 scenario is run 1000 times for various SCR and shape parameters while the false alarm is fixed as
 229 $P_{FA} = 10^{-3}$.

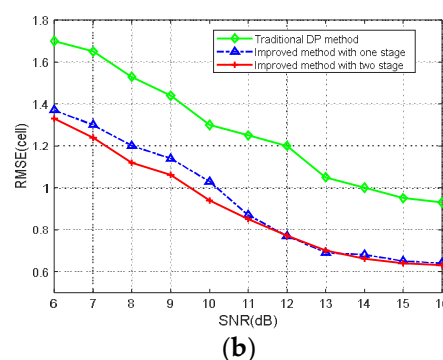
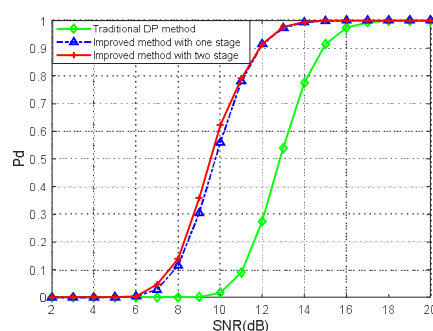
230 4.1. Performance Analysis

231 We assess the performances of different strategies via the probability of track detection P_d , which
 232 is a performance metric for both detection and tracking performance. P_d is defined as the probability
 233 of the maximum integration value exceeding detection threshold, and its final position is within
 234 certain range of the actual target position. In addition, the root-mean square error (RMSE) on the
 235 estimation of the target position is also considered, which is defined as

$$RMSE = \sqrt{E[e^2(s_n)|H_1]} \quad (21)$$

236 where H_1 is the event that target is confirmed, and $e^2(s_n)$ is the Euclidean distance between the
 237 true and estimated target position.

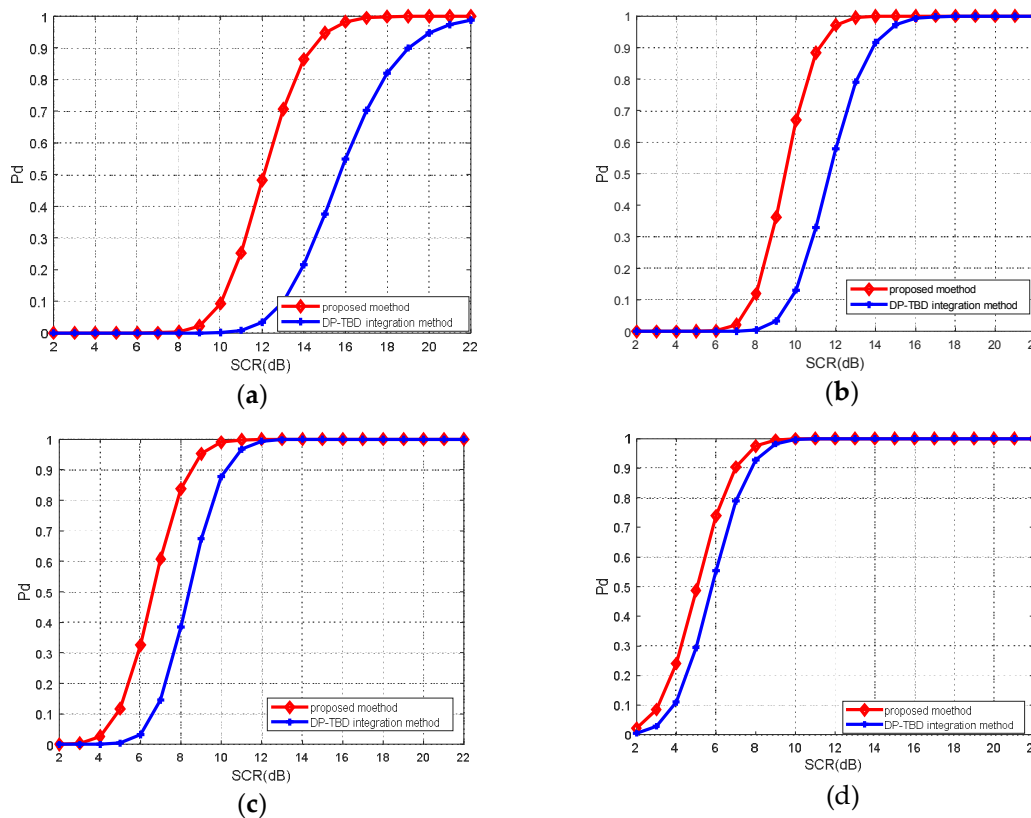
238 Performance and RMSE comparison of conventional DP method and proposed method based
 239 on prior information is shown in Figure 6. For K-distributed clutter and Swerling 1 target, proposed
 240 method performs better than the traditional integration method. It can also be concluded that for
 241 proposed method, which processed with only one stage (blue solid line) or two-stage (red solid line)
 242 could achieve almost identical performance while the latter one obtains further computational
 243 reduction.



(a)

244 **Figure 6.** Performance and RMSE comparison of different DP-TBD integration method with
 245 $\alpha=0.5$ and $\beta=1$ against SNRs from 2dB to 20dB (a) The detection probability P_d (b) The RMSE on
 246 estimated position.

247 For different parameters of K-distributed clutter, detection performances are shown in Figure 8.
 248 With the increasing of shape parameter α , both conventional DP and proposed method on prior
 249 information, achieve significant performance improvement. That's because when α is increasing, the
 250 K-distributed clutter is smoother and the frequency of target-like outliers is lower. Note that when α
 251 = 50, since K distribution almost degenerates to Rayleigh distribution in this case, the detection
 252 performances are nearly identical.



253 **Figure 7.** Performance comparison of DP-TBD integration method (red solid line with diamond) and
 254 proposed method in this paper (blue solid line with cross) for K-distributed clutter and Swerling 1
 255 target (a). $\alpha=2$ and $\beta=2$; (b). $\alpha=5$ and $\beta=2$; (c). $\alpha=10$ and $\beta=2$; (d). $\alpha=50$ and $\beta=2$;

256 4.2. Computational Complexity Analysis

257 The complexity of the conventional DP-TBD method is $\mathcal{O}(M_r M_\theta q N)$, where M_r and M_θ are
 258 the number of range and azimuth resolution elements, q is the number of possible state transition in
 259 a scan and N is the number of the integration scans. In comparison with the conventional method,
 260 the two-stage detection approach schemed in Figure 3 has low computational complexity. The
 261 computational cost in stage 1 is $\mathcal{O}(M'_r M'_\theta q N)$, where $M'_r \times M'_\theta$ denotes grid cells re-discretized by
 262 $\Delta r'$ and $\Delta \theta'$ to realize the target search with larger cell size. Since the DP integration in stage 2 is
 263 concentrated on the part of states, which are indicated by stage 1, the computational cost is small
 264 enough to be neglected.
 265

266

Table 1. Computational cost with different parameters

Parameters	$M_r \times M_\theta = 180 \times 90$	$M'_r \times M'_\theta = 90 \times 45$	$M''_r \times M''_\theta = 60 \times 30$
q=4	308ms	224ms	146ms
q=9	935ms	684ms	370ms

267

268

269

270

271

272

273

The computational cost of strategies is listed in Table 1 for different parameters. It can be seen that the computational cost depends on the number of possible state transition q and the resolution elements. For the same resolution cells, scenario at $q=9$ costs almost three times as long as the scenario $q=4$. Meanwhile, the computational cost reduces rapidly as the number of resolution elements decreases. For example, when $q=4$, the CPU times for $M_r \times M_\theta = 180 \times 90$, $M'_r \times M'_\theta = 90 \times 45$ and $M''_r \times M''_\theta = 60 \times 30$ are 308ms, 224ms and 146ms, respectively.

274

5. Conclusion

275

276

277

278

279

280

281

282

283

284

285

286

287

288

This paper has presented the systematic treatment of heavy-tailed clutter from a target detection and tracking perspective. Target detection in K-distributed clutter is more challenging than in Gaussian- or Rayleigh-distributed clutter due to the higher likelihood of target-like outliers, especially for fluctuating target. In this work, we dealt with the fluctuating target detection and tracking problem using modified DP-TBD method. The contributions are as follows: First we have solved the target detection problem using two-stage detection architecture to avoid calculations of less meaningful states. Secondly, for Swerling 1 target in K-distributed background, merit function was derived and implemented in the integration process of DP-TBD to enhance radar detection performance. In order to reduce the complexity of integral calculation, we also resorted to the trapezoidal rule with a generating lookup table.

Numerical analysis demonstrated that performance improvement could be applied via proposed DP-TBD algorithm based on prior information, especially for heavy-tailed K-distributed clutter. Moreover, simulation results suggested that a tradeoff between performance and computational complexity exists.

289

290

291

Acknowledgments: This work was supported by the National Key Research and Development Program of China (Grant No. 2016YFB0101101), by the National Natural Science Foundation of China (Grant No. 61703393 and No. U1613214).

292

293

294

Author Contributions: Jie Gao contributed to the original ideas and designed the simulations; Jie Gao and Wei Wang performed the simulations and analyzed the data; Jinsong Du provided the significant guidance in research planning and revised the manuscript. All authors contributed to and approved the written manuscript.

295

Conflicts of Interest: The authors declare no conflict of interest.

296

References

297

298

299

300

301

302

303

304

305

306

1. Barniv, Y.; Kella, O., Dynamic Programming Solution for Detecting Dim Moving Targets Part II: Analysis. *IEEE Transactions on Aerospace & Electronic Systems* **1985**, *21* (1), 144-156.
2. Barniv, Y.; Kella, O., Dynamic Programming Solution for Detecting Dim Moving Targets Part II: Analysis. *IEEE Transactions on Aerospace and Electronic Systems* **1987**, *AES-23* (6), 776-788.
3. Buzzi, S.; Lops, M.; Venturino, L.; Ferri, M. In *Detection of an Unknown Number of Targets via Track-Before-Detect Procedures*, 2007 IEEE Radar Conference, 17-20 April 2007; 2007; pp 180-185.
4. Buzzi, S.; Lops, M.; Venturino, L.; Ferri, M., Track-before-detect procedures in a multi-target environment. *IEEE Transactions on Aerospace and Electronic Systems* **2008**, *44* (3), 1135-1150.
5. Yi, W.; Morelande, M. R.; Kong, L.; Yang, J., An efficient multi-frame track-before-detect algorithm for multi-target tracking. *IEEE Journal on Selected Topics in Signal Processing* **2013**, *7* (3), 421-434.

- 307 6. Grossi, E.; Lops, M.; Venturino, L. In *A track-before-detect procedure for sparse data*, 2012 IEEE Statistical Signal
308 Processing Workshop (SSP), 5-8 Aug. 2012; 2012; pp 772-775.
- 309 7. Grossi, E.; Lops, M.; Venturino, L. In *A novel track-before-detect procedure for multi-frame detection in radar*
310 *systems*, 2013 IEEE Radar Conference (RadarCon13), April 29 2013-May 3 2013; 2013; pp 1-6.
- 311 8. Jiang, H.; Yi, W.; Cui, G.; Kong, L.; Yang, X. In *Track-before-detect strategy for HRR radars*, 2015 IEEE
312 International Radar Conference, RadarCon 2015, May 10, 2015 - May 15, 2015, Arlington, VA, United states,
313 Institute of Electrical and Electronics Engineers Inc.: Arlington, VA, United states, 2015; pp 362-367.
- 314 9. Jiang, H.; Yi, W.; Kong, L.; Yang, X.; He, B. In *Radar detection of Swerling 3 target in G0-distributed clutter via*
315 *track-before-detect*, 2016 IEEE Radar Conference, RadarConf 2016, May 2, 2016 - May 6, 2016, Philadelphia,
316 PA, United states, Institute of Electrical and Electronics Engineers Inc.: Philadelphia, PA, United states,
317 2016; p IEEE AESS; Philadelphia Section of the IEEE.
- 318 10. Yi, W.; Jiang, H.; Kirubarajan, T.; Kong, L.; Yang, X., Track-Before-Detect Strategies for Radar Detection in
319 G0-Distributed Clutter. *IEEE Transactions on Aerospace and Electronic Systems* **2017**, *53* (5), 2516-2533.
- 320 11. Buzzi, S.; Lops, M.; Venturino, L., Track-before-detect procedures for early detection of moving target from
321 airborne radars. *IEEE Transactions on Aerospace & Electronic Systems* **2005**, *41* (3), 937-954.
- 322 12. Ebenezer, S. P.; Papandreou-Suppappola, A., Generalized Recursive Track-Before-Detect With Proposal
323 Partitioning for Tracking Varying Number of Multiple Targets in Low SNR. *IEEE Transactions on Signal*
324 *Processing* **2016**, *64* (11), 2819-2834.
- 325 13. Zheng, D.; Wang, S.; Qin, X., A Dynamic Programming Track-Before-Detect Algorithm Based on Local
326 Linearization for Non-Gaussian Clutter Background. *Chinese Journal of Electronics* **2016**, *25* (3), 583-590.
- 327 14. Zhou, J.; Chen, D.; Sun, D. In *K Distribution Sea Clutter Modeling and Simulation Based on ZMNL*, International
328 Conference on Intelligent Computation Technology and Automation, 2016; pp 506-509.
- 329 15. Aprile, A.; Grossi, E.; Lops, M.; Venturino, L., Track-before-detect for sea clutter rejection: tests with real
330 data. *IEEE Transactions on Aerospace and Electronic Systems* **2016**, *52* (3), 1035-1045.
- 331 16. Berry, P.; Venkataraman, K.; Rosenberg, L. In *Adaptive detection of low-observable targets in correlated sea clutter*
332 *using Bayesian track-before-detect*, Radar Conference, 2017; pp 0398-0403.
- 333 17. Swerling, P., Probability of detection for fluctuating targets. *Information Theory Ire Transactions on* **1960**, *IT-*
334 *6* (2), 269-308.
- 335 18. Brekke, E.; Hallingstad, O.; Glattetre, J., Tracking Small Targets in Heavy-Tailed Clutter Using Amplitude
336 Information. *IEEE Journal of Oceanic Engineering* **2010**, *35* (2), 314-329.
- 337 19. Abraham, D. A.; Lyons, A. P., Novel physical interpretations of K-distributed reverberation. *Oceanic*
338 *Engineering IEEE Journal of* **2002**, *27* (4), 800-813.

339

340